On the Sol-gel Preparation of Selected Lanthanide Aluminium Garnets Doped with Europium

L. Pavasaryte[1], B. J. Lopez[2] and A. Kareiva[1]
[1]*Department of Inorganic Chemistry, Vilnius University, Naugarduko 24, LT-03225 Vilnius, Lithuania*
[2]*Departament de Química Inorgànica i Orgànica, Universitat Jaume I, E-12071 Castelló de la Plana, Spain*

Keywords: Lanthanide Aluminium Garnets, Holmium, Terbium, Dysprosium, Doping, Europium, Sol-gel Processing, XRD, FTIR, SEM, DLS, Fluorescence.

Abstract: A sol-gel method based on in-situ generation of mixed-metal chelates by complexing metal ions with ethane-1,2-diol in an aqueous media has been elaborated to prepare lanthanide-ion containing garnets, $Tb_3Al_5O_{12}$ (TAG), $Dy_3Al_5O_{12}$ (DAG) and $Ho_3Al_5O_{12}$ (HAG) doped with different amount of Eu. The X-ray diffraction patterns (XRD) of the powders sintered at 1000 °C showed the formation of monophasic TAG, DAG and HAG. The phase composition of the samples was also characterized by FTIR spectroscopy. Microstructural features of the polycrystalline samples were studied by scanning electron microscopy (SEM) and dynamic light scattered measurements (DLS). Luminescence properties were investigated by laser and fluorescence spectrophotometer.

1 INTRODUCTION

The yttrium aluminium garnet ($Y_3Al_5O_{12}$, YAG) doped with a transition metal or lanthanide ions is an important solid-state laser material widely used in luminescence systems, window materials for a variety of light sources, and for fiber-optic telecommunication systems. The YAG oxides are also widely applied as phosphors in cathode-ray tubes (projection TV sets), field emission, vacuum fluorescent, and electroluminescent displays and as scintillators in X-ray and positron emission tomographs (Harlan et al. 1997; Vaqueiro et al. 1998; Pullar et al. 1999; Ganschow et al. 1999; Kang et al. 1999; Lu et al. 2000; Lu et al. 2002; Hreniak et al. 2002; Pan et al. 2004; Potdevin et al. 2006; Singh et al. 2007; Katelnikovas et al. 2007; Caponetti et al. 2007; Caponetti et al. 2007; Lipinska et al. 2007; Katelnikovas et al. 2008; Khimich et al. 2009; Suarez et al. 2009; Yang et al. 2009; Sun et al. 2009; Fujioka et al. 2009; Yang et al. 2010). These features have made rare-earth-doped YAG a relevant material for cathode-ray tubes (CRTs), field emission displays (FED), vacuum fluorescent and electroluminescent displays, plasma display panel, scintillators in X-ray and positron emission tomographs and other luminescent applications.

The phosphors host materials have proven to be of great importance for the optical function. The matrix should possess good chemical, mechanical, thermal, optical characteristics and properties. It is well known that physical properties of crystalline materials are very dependent on the host material, phase purity, distribution of the grains sizes and crystalline homogeneity. (Iida et al. 1999; Golubovic et al. 2002; Zhang et al. 2008). For example, transition metal and rare-earth element ions have demonstrated lasing action in a wide variety of host crystals. Among the compounds which can incorporate transition metals or lanthanides several scandium and gallium based materials were elaborated (Vosegaard et al. 1997; Ferrand et al. 1999; Gaume et al. 2003; Muliuoliene et al. 2003; Chenais et al. 2003; Garskaite et al. 2005; Mathur et al. 2005; Sakirzanovas et al. 2008; Katelnikovas et al. 2008). In the YAG all aluminium ions may be substituted by gallium or iron ions, while pure yttrium indium or yttrium scandium garnet is not obtained. Besides, rare-earth aluminium garnets have also attracted considerable attention as host crystals for near-infrared solid-state lasers as well as for optoelectronics devices, including computer memories, microwave optical elements and as laser active media with applications in medical surgery, optical communications and coherent laser radar (Papagelis et al. 2002; Papagelis et al. 2003; Milanese et al. 2004).

Many different synthesis methods of synthetic garnets are described in the literature. The solid-state

Pavasaryte L., Lopez B. and Kareiva A..
On the Sol-gel Preparation of Selected Lanthanide Aluminium Garnets Doped with Europium.
DOI: 10.5220/0005252901650171
In *Proceedings of the 3rd International Conference on Photonics, Optics and Laser Technology* (PHOTOPTICS-2015), pages 165-171
ISBN: 978-989-758-093-2

reaction route is a widely used method for the preparation of powders from a mixture of the solid starting materials. Various wet-chemical methods, which include combustion, co-precipitation, hydrothermal, spray pyrolysis, sol-gel and emulsion synthesis method have been developed and successfully used for a low-temperature production of phase-pure YAG, YGG, YIG powders and related systems. Recently we have demonstrated that monophasic yttrium aluminium garnet powders and related garnet structure compounds with homogeneously distributed lanthanide elements within the garnet matrix can be successfully synthesized by the simple aqueous sol-gel process. The evaluated synthetic technique to garnet structure compounds using acetate-nitrate-glycolate intermediate illustrates the simplicity and superior potential of the proposed method (Katelnikovas et al. 2007; Kareiva 2011; Skaudzius et al. 2014; Zabiliute et al. 2014). The molecular level mixing and the tendency of partially hydrolyzed species to form extended networks facilitate the structure evolution thereby lowering the crystallization temperature. The reactivity of such precursors makes the preparation of particular phases possible at ambient and gentle conditions (Livage et al. 1988; Brinker et al. 1990; Cushing et al. 2004; Mackenzie et al. 2007; Dubnikova et al. 2010).

Several lanthanide aluminium garnets (i.e., $Tb_3Al_5O_{12}$, $Dy_3Al_5O_{12}$ and $Ho_3Al_5O_{12}$) had not been synthesized with various doping level of europium using an aqueous sol-gel technique, to the best our knowledge. Therefore, the main aim of this study was to prepare $Tb_3Al_5O_{12}:Eu^{3+}$, $Dy_3Al_5O_{12}:Eu^{3+}$ and $Ho_3Al_5O_{12}:Eu^{3+}$ using sol-gel technique and investigate luminescent properties of these Eu^{3+}-doped garnets.

2 EXPERIMENTAL

The lanthanide aluminium garnet samples were synthesized by an aqueous sol-gel method with optimized synthesis parameters by mathematical regression model (Katelnikovas et al. 2007; Dubnikova et al. 2010). In the aqueous sol-gel process, the following materials were used: Ho_2O_3 (99.9 %), Tb_4O_7 (99.9 %), Dy_2O_3 (99.99%) and Eu_2O_3 (99.99%). Ho, Dy and Tb oxides were dissolved in nitric acid (about 10 ml) with small amount of water. Clear solutions were obtained after stirring at 60-65 °C in beakers covered with a watch-glass till dissolved. When oxides dissolved, mixture washed with water till neutral pH. Then aluminium nitrate nonahydrate and appropriate amount of europium oxide dissolved in small amount of nitric acid were added to above solutions and diluted till 100 ml. The resulting mixtures were stirred at 65 °C for 1 h, followed by dropwice addition of ethane-1,2-diol ($HOCH_2CH_2OH$) upon vigorous stirring. The resulting sols were mixed at the same temperature for another 1 h and then concentrated by slow solvent evaporation at 65 °C until they turned into transparent gels. The gels were dried in an oven at 100 °C for 24 h. The resulting gel powders were ground in an agate mortar and heated in air at 800 °C for 4 h by slow temperature elevation (5 °C min^{-1}). After grinding in an agate mortar, the powders were further sintered in air at 1000 °C temperature for 10h.

The synthesized samples were characterized by X-ray powder diffraction (XRD) analysis, Fourier transform infrared (FTIR) spectroscopy, scanning electron microscopy (SEM), fluorescence spectroscopy (FS) and dynamic light scattered measurement (DLS). The XRD studies were performed on D8 Bruker AXS powder diffractometer using CuKα1 radiation. The diffraction patterns were recorded at the standard rate of 1.5 2θ / min. The FTIR spectra were recorded with a Perkin-Elmer FT-IR Spectrum 1000 spectrometer. The scanning electron microscope DSN 962 was used to study the surface morphology and microstructure of the obtained ceramic samples. Fluorescence data characterized by fluorescence spectrophotometer Cary Eclipse Varian. Particle size were identified by Zetasizer, nano series.

3 RESULTS AND DISCUSSION

3.1 XRD Characterization of LnAG:Eu Powders

The phase purity and compositional changes of the LnAG doped with different amount of Eu ions were controlled by X-ray diffraction analysis. The XRD patterns of corresponding $Tb_3Al_5O_{12}$ (TAG), $Dy_3Al_5O_{12}$ (DAG) and $Ho_3Al_5O_{12}$ (HAG), with different doping level of Eu powders annealed at 1000 ^oC are shown in Figs. 1-3, respectively.

The XRD results presented in Fig. 1 revealed that ceramics obtained at 1000 °C consists of one crystalline phase: terbium aluminium garnet ($Tb_3Al_5O_{12}$, TAG). The obtained XRD patterns are in a good agreement with the reference data for $Tb_3Al_5O_{12}$ (PDF [04-006-4054]). Fig. 2 shows that only one dysprosium aluminium garnet $Dy_3Al_5O_{12}$

phase (PDF [04-006-4053]) was obtained after calcination of Dy-Al-O:Eu precursors at 1000 °C. In the case of the Ho-Al-O system, the analogous results with of the Tb-Al-O and Dy-Al-O systems were obtained. In Fig. 3 the X-ray diffraction patterns of the final Ho-Al-O ceramic samples annealed at 1000 °C are presented. The XRD patterns prove the formation of the cubic holmium aluminium garnets ($Ho_3Al_5O_{12}$). Evidently, the obtained XRD patterns are in a good agreement with the reference data for $Ho_3Al_5O_{12}$ (PDF [04-001-9715]). Thus, we can conclude that the 1000 °C temperature is enough for the formation of Eu^{3+}-doped $Tb_3Al_5O_{12}$, $Dy_3Al_5O_{12}$ and $Ho_3Al_5O_{12}$ garnets.

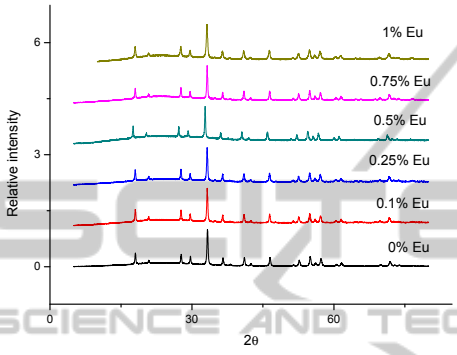

Figure 1: XRD patterns of the Tb-Al-O:Eu gels annealed at 1000 °C.

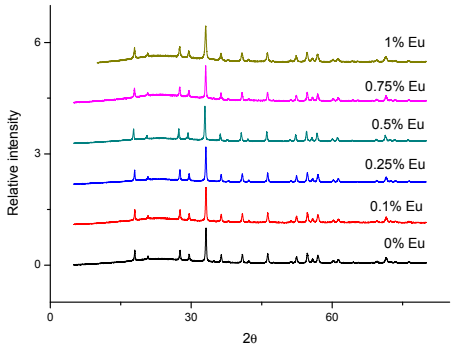

Figure 2: XRD patterns of the Dy-Al-O:Eu gels annealed at 1000 °C.

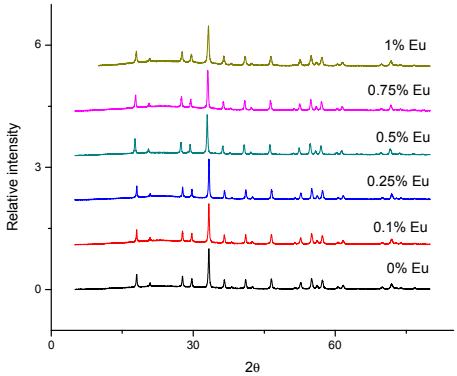

Figure 3: XRD patterns of the Ho-Al-O:Eu gels annealed at 1000 °C.

3.2 Infrared Spectroscopy

FTIR spectroscopy was used as additional tool for the structural characterization of the ceramic materials obtained by the aqueous sol-gel method. The FTIR spectra of ceramic materials obtained after the calcinations of the Ho-Al-O:Eu gels at 1000 °C for 10 h are shown in Fig. 4.

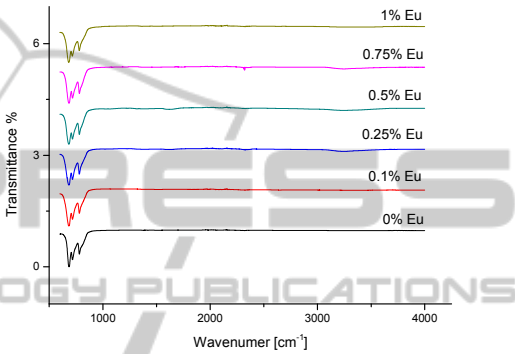

Figure 4: FTIR spectra of $Ho_3Al_5O_{12}:Eu^{3+}$ garnets synthesized at 1000 °C.

The FTIR spectra of synthesized ceramics show several quite intense broad bands at 675 cm^{-1}, 720 cm^{-1} and 775 cm^{-1}, which are typical metal-oxygen (M-O) absorptions for the garnet-type compounds (Dubnikova et al. 2010; Garskaite et al. 2010; Li et al. 2005). The FTIR spectra of Tb-Al-O and Dy-Al-O garnets doped with europium were very similar to the presented in Fig. 4. The most important feature is that intensive bands are determined in the region of 900–450 cm^{-1}, which may be also attributed to the stretching modes of the isolated [AlO_4] tetrahedra and [AlO_6] octahedra in the garnet structure, i.e. these bands correspond to the formation of crystalline TAG:Eu, DAG:Eu and HAG:Eu. Thus, the observed M–O vibrations which in view of the earlier reports are characteristic of RE–O and Al–O stretching frequencies let us to conclude, that the FTIR results are consistent with crystallization process observed by XRD measurements. Consequently, the FTIR results absolutely support the conclusions made on grounds of the XRD measurement and prove that there is no left organic matter in the sol-gel derived garnet structure compounds (Li et al. 2005; Li et al. 2004; Xing et al. 2004; Pralad et al. 2013).

3.3 Scanning Electron Microscopy

The textural properties of the calcined Tb-Al-O:Eu, Dy-Al-O:Eu, Ho-Al-O:Eu powders were investigated by SEM, from which the grain size and typical morphologies were obtained. Scanning electron micrographs of the Tb-Al-O:0.5%Eu, Dy-Al-O:0.5%Eu and Ho-Al-O:0.5%Eu samples calcined at 1000 ºC are shown in Figs. 5-7, respectively. The SEM once again proved to be a valuable technique for the morphological characterization of ceramic samples. Individual particles seem to be submicro-sized plate-like crystals and they partially fused to form hard agglomerates. The SEM micrograph presented in Fig. 5 shows the formation of very homogeneous mixed-metal oxide, and the formation of a continuous network of crystallites is characteristic feature for ceramic composite material during calcination. The Ho-Al-O:Eu and Dy-Al-O:Eu garnet particles are a little differently shaped comparing with Tb-Al-O:Eu garnet (see Figs. 6 and 7). Apparently, the particles were formed with more pronounced agglomeration, indicating good connectivity between the grains which is characteristic feature for ceramic composite material (Skaudzius et al. 2008).

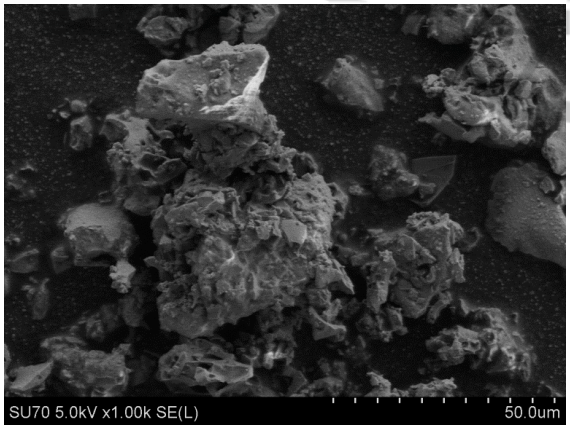

Figure 5: SEM micrograph of the $Tb_3Al_5O_{12}$:0.5% Eu^{3+} garnet.

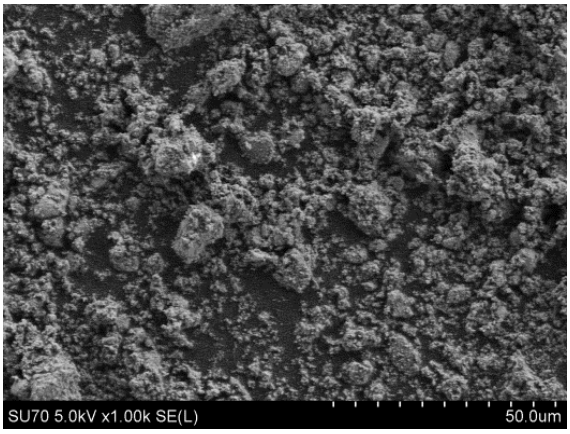

Figure 6: SEM micrograph of the $Dy_3Al_5O_{12}$:0.5% Eu^{3+} garnet.

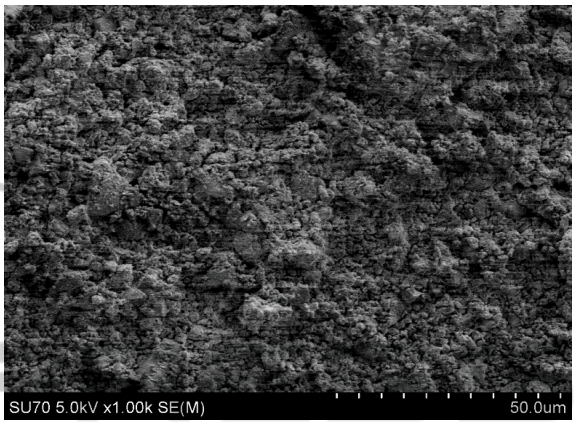

Figure 7: SEM micrograph of the $Ho_3Al_5O_{12}$:0.5% Eu^{3+} garnet.

3.4 Dynamic Light Scattered Measurements

The particle size distribution in $Ho_3Al_5O_{12}$:Eu garnets annealed at 1000 °C for 10 h were investigated by dynamic light scattering (DLS). The DLS measurements showed well size distribution of garnets. When Eu doping level les or equal 0.1% possible very narrow particle size distribution (~420 nm) was determined. The sample with higher europium concentration (0.5%) were composed with larger particles (~700 nm). When garnet doped with 0.25% - 0.75% of Eu^{3+} some particles were much more larger, and consequently the particle size is not stable and split in a biggest range. However, the biggest particle size was determined for the sample with 1% of doping level of Eu. Interestingly, the DLS results fit very well with scanning electron microscopy data showing that 0.5% of Eu is the optimum doping level for Tb, Dy and Ho aluminium garnets having very homogeneous particle size distribution.

3.5 Optical Properties

The fluorescence data of $Ho_3Al_5O_{12}$:Eu are shown in Fig. 8.

As seen. the 0.5% Eu-doped sample shows the most intensive europium peaks between investigated the Ho-Al-O:Eu garnet structure compounds.

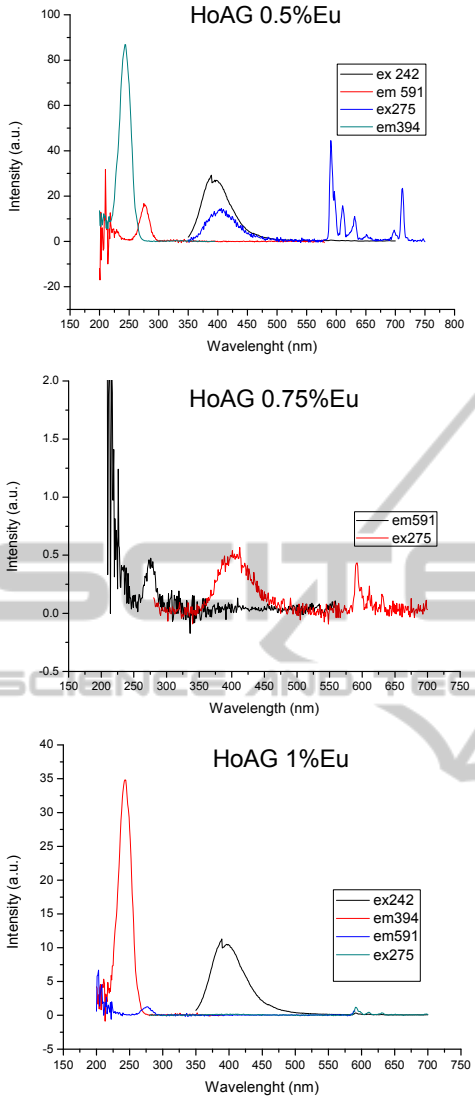

Figure 8: Fluorescence measurement data of $Ho_3Al_5O_{12}:Eu^{3+}$ garnets.

This data fit well with XRD results (peaks with 0,5% europium are shifted to the smaller 2θ). The sample having 1% of Eu shows possible fluorescence, however, not so intensive as with 0.5% of Eu, but more intensive than 0.75% Eu-doped sample. The XRD data also showed the smaller shift for 0.75% Eu and 1% Eu samples. Finally, the results of fluorescence measurement support the proposition that the best doping level for HAG:Eu is 0.5% of europium.

It is particularly well known that, phosphors with spherical shaped particles (≤ 2 μm) are of greater importance because of their high packing density, lower scattering of light, brighter luminescent performance, high definition and more improved screen packing density. This explain why 0.5 europium doping shows the best luminescent properties (Raju et al. 2008; Park et al. 2010).

Figs. 9 and 10 represent luminescence spectra of $Tb_3Al_5O_{12}:Eu$ and $Dy_3Al_5O_{12}:Eu$ garnets, respectively.

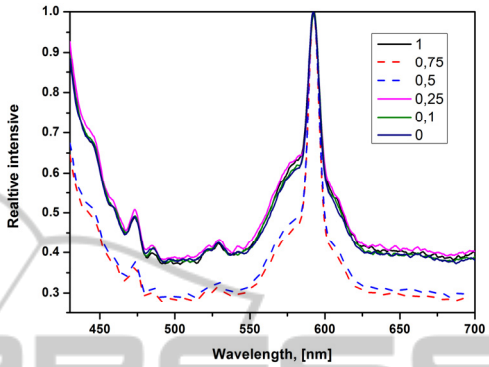

Figure 9: Luminescent (emission) spectra of $Tb_3Al_5O_{12}:Eu^{3+}$ garnets.

The spectra were acquired by using 394 nm and 275 nm excitation. The emission peaks were fixed between 550 and 650 nm, and well agree with the reported values of Eu^{3+} emission transitions [56-58]. The emission spectral lines of Eu^{3+} ion are sharp which is due to the screening of 4f orbital by 5s and 5p orbitals from crystal field of the host lattice.

Spectrums show the characteristic emission of Eu^{3+} arising due to $^5D_0 \rightarrow {}^7F_1$ (591nm), $^5D_0 \rightarrow {}^7F_2$ (611nm) and $^5D_0 \rightarrow {}^7F_4$ (708nm) transitions (Singh et al. 2013). As expected for the Eu^{3+} ions a typical strong red emission was present with the most intense line at 611 nm originated from the $^5D_0 \rightarrow {}^7F_2$ hypersensitive transition (Redenka et al. 2014). Few of $Ho_3Al_5O_{12}:Eu$ doping (0.1% Eu, 0.25% Eu) do not show any emission peaks. The results obtained are in a good agreement with fluorescence data, beside with this doping level peaks in XRD graphs did not shift.

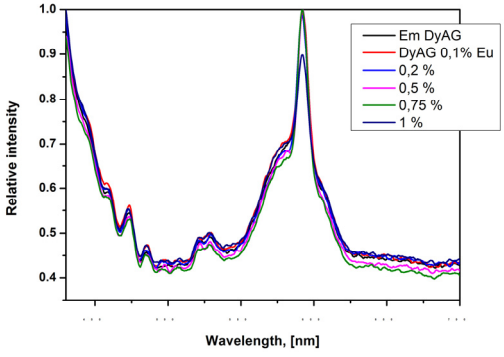

Figure 10: Luminescent (emission) spectra of $Dy_3Al_5O_{12}:Eu^{3+}$ garnets.

Fig. 11: represents the life time of $Ho_3Al_5O_{12}$:Eu garnets obtained after annealing at 1000 °C for 10 h.

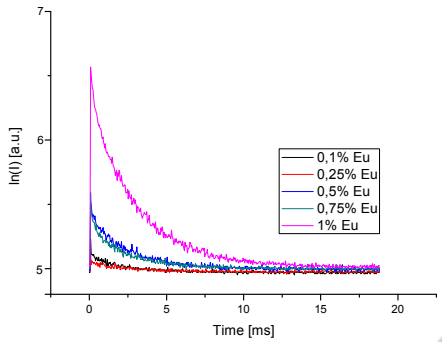

Figure 11: The life time measurements for the $Ho_3Al_5O_{12}:Eu^{3+}$ garnets.

The luminescence lifetime for the most intense emission line at 611 nm of Eu^{3+} ($^5D_0 \rightarrow {}^7F_1$) were recorded using 275 nm as excitation source. The obtained photoluminescence lifetimes show a decrease (Fig. 12) from 2.58 to 1.98 ms with increasing doping concentration. Upon increasing the doping concentration, the decay becomes faster. In our case the maximum decay time is 2.58 ms with 0,1 mol% doping concentration. Increasing doping content may increase the number of ions occupying the surface states in nanoscale dimensional materials and these states may be leading to concentration – quenching behaviour (Packiyaraj et al. 2014; Muenchausen et al. 2007). Decay time decrease with increasing doping content. This result supports emission and excitation spectral analysis.

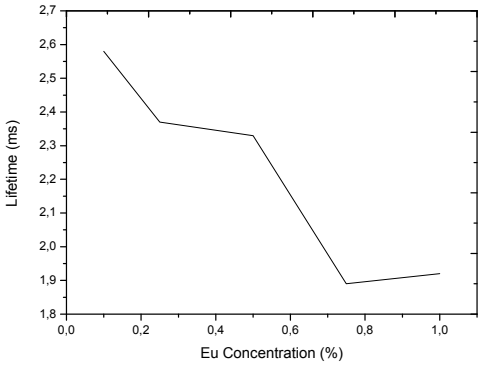

Figure 12: The decay curves for $Ho_3Al_5O_{12}:Eu^{3+}$ garnet.

4 CONCLUSIONS

The sinterability and microstructal evolution of synthesized lanthanide aluminium garnets by an aqueous sol-gel process were investigated in the present study. In this work aqueous sol-gel process was used to prepare lanthanide-aluminium oxides $Tb_3Al_5O_{12}$, $Dy_3Al_5O_{12}$ and $Ho_3Al_5O_{12}$ doped with different amount of europium. It was concluded from the XRD data that monophasic $Tb_3Al_5O_{12}$:Eu, $Dy_3Al_5O_{12}$:Eu and $Ho_3Al_5O_{12}$:Eu garnets can be easily synthesized at 1000 °C using the proposed sol-gel chemistry approach. Europium inside garnet structure slightly shifted the reflection peaks in the XRD patterns. The biggest shift was observed in the XRD pattern of the samples with 0.5% of Eu. The XRD results were supported by FTIR, SEM, DLS fluorescence and luminescent measurements. It was also determined that the amount of europium inside garnet structure influenced the particle size. With increasing doping level the particle size also increased. The luminescence lifetime for the most intense emission line at 611 nm of Eu^{3+} ($^5D_0 \rightarrow {}^7F_1$) was recorded using 275 nm as excitation source in HAG and 394 nm in TAG and DAG. Upon increasing the doping concentration, the decay became faster in $Ho_3Al_5O_{12}$:Eu. The characterization of synthesized samples using all measurements used in this study resulted to the conclusion that that 0.5% of europium is optimum doping level. Thus, the developed synthesis route offers unique opportunities for the synthesis of optical materials, since it is suited for the production of thin/thick films, monoliths and fibbers.

REFERENCES

C. J. Harlan, A. Kareiva, D. B. MacQueen, R. Cook, and A. R. Barron, 1997. Adv. Mater. 9, 68.
P. Vaqueiro, and M. A. Lopez-Quintela, 1998. J. Mater. Chem. 8, 161 (1998).
R. C. Pullar, M. D. Taylor, and A. K. Bhattacharya, 1999. J. Eur. Ceram. Soc. 19, 1747.
S. Ganschow, D. Klimm, P. Reiche, and R. Uecker, 1999. Cryst. Res. Technol. 34, 615.
Y. C. Kang, I. W. Lenggoro, S. B. Park, and K. Okuyama, 1999. J. Phys. Chem. Solids 60, 1855.
J. Lu, M. Prabhu, J. Song, C. Li, J. Xu, K. Ueda, A. A. Kaminskii, H. Yagi, and T. Yanagitani, 2000. Appl. Phys. B 71, 469.
C. H. Lu, H. C. Hong, and R. Jagannathan, 2002. J. Mater. Chem. 12, 2525.
D. Hreniak, and W. Strek, 2002. J. All. Comp. 341, 183.
Y. Zhou, J. Lin, M. Yu, S. Wang, and H. Zhang, 2002. Mater. Lett. 56, 628.
Y. Pan, M. Wu, and Q. Su, 2004. J. Phys. Chem. Solids 65, 845.
A. Potdevin, G. Chadeyron, D. Boyer, and R. Mahiou, 2006. J. Sol-Gel Sci. Techn. 39, 275.
R. Singh, R. K. Khardekar, A. Kumar, and D. K. Kohli, 2007. Mater. Lett. 61, 921.

A. Katelnikovas, P. Vitta, P. Pobedinskas, G. Tamulaitis, A. Zukauskas, J.-E. Jørgensen, and A. Kareiva, 2007. J. Cryst. Growth 304, 361.
E. Caponetti, M. L. Saladino, F. Serra, and S. Enzo, 2007. J. Mater. Sci. 42, 4418.
E. Caponetti, S. Enzo, B. Lasio, and M. L. Saladino, 2007 Opt. Mater. 29, 1240.
L. Lipinska, L. Lojko, A. Klos, S. Ganschow, R. Diduszko, W. Ryba-Romanowski, and A. Pajaczkowska, 2007. J. All. Comp. 432, 177.
A. Katelnikovas, T. Justel, D. Uhlich, J.-E. Jorgensen, S. Sakirzanovas, and A. Kareiva. 2008. Chem. Eng. Comm. 195, 758.
N. N. Khimich, E. N. Poddenezhnyi, A. A. Boiko, A. V. Zdravkov, V. L. Ugolkov, L. A. Koptelova, E. I. Grishkova, and A. O. Dobrodei, 2009. Glass Phys. Chem. 35, 504.
M. Suarez, A. Fernandez, J. L. Menendez, and R. Torrecillas, 2009. J. Nanomater. Art. # 138490.
H. J. Yang, L. Yuan, G. S. Zhu, A. B. Yu, and H. R. Xu, 2009. Mater. Lett. 63, 2271.
X. X. Ge, Y. H. Sun, C. Liu, and W. K. Qi, 2009. J. Sol-Gel Sci. Technol. 52, 179.
K. Fujioka, T. Saiki, S. Motokoshi, Y. Fujimoto, H. Fujita, and M. Nakatsuka, 2009. Ceram. Int. 35, 2393.
H. K. Yang, and J. H. Jeong, 2010. J. Phys. Chem. C 114, 226.
Y. Iida, A. Towata, T. Tsugoshi, and M.Furukawa, 1999. Vibr. Spectr. 19, 399.
A. Golubovic, S. Nikolic, R. Gajic, S. Duric, and A. Valcic, 2002. J. Serb. Chem. Soc. 67, 291.
L. Zhang, C. Y. Zhang, D. H. Li, Z. Y. Wei, Z. G. Zhang, J. E. Hans, and S. Strohmaier, 2008. Chin. Phys. Lett. 25, 3988.
T. Vosegaard, D. Massiot, N. Gautier, and H. J. Jakobsen, 1997. Inorg. Chem. 36, 2446.
B. Ferrand, B. Chambaz, and M. Couchaud, 1999. Opt. Mater. 11, 101.
R. Gaume, B. Viana, J. Derouet, and D. Vivien, 2003. Opt. Mater. 22, 107.
I. Muliuoliene, S. Mathur, D. Jasaitis, H. Shen, V. Sivakov, R. Rapalaviciute, A. Beganskiene, and A. Kareiva, 2003. Opt. Mater. 22, 241.
S. Chenais, F. Druon, F. Balembois, P. Georges, A. Brenier, and G. Boulon, 2003. Opt. Mater. 22 99.
E. Garskaite, Z. Moravec, J. Pinkas, S. Mathur, R. Kazlauskas, and A. Kareiva, 2005. Phil. Magaz. Lett. 85, 557.
S. Mathur, H. Shen, A. Leleckaite, A. Beganskiene, and A. Kareiva, 2005. Mater. Res. Bull. 40, 439.
S. Sakirzanovas, L. Sun, Ch. Yan, and A. Kareiva, 2008. Mendeleev Commun. 18, 251.
A. Katelnikovas, and A. Kareiva. 2008. Mater. Lett. 62, 1655.
K. Papagelis, G. Kanellis, T. Zorba, S. Ves, and G. A. Kourouklis, 2002. J. Phys. Condens. Matter 14, 915.
K. Papagelis, and S. Ves, 2003. J. Phys. Chem. Solids 64, 599.
C. Milanese, V. Buscaglia, F. Maglia, and U. Anselmo-Tamburini, 2004. Chem. Mater. 16, 1232.
A. Katelnikovas, J. Barkauskas, F. Ivanauskas, A. Beganskiene, and A. Kareiva, 2007. J. Sol-Gel Sci. Techn. 41, 193.
A. Kareiva, 2011. Materials Science (Medžiagotyra), 17, 428.
R. Skaudzius, A. Katelnikovas, D. Enseling, A. Kareiva, and T. Juestel, J. Lumin. 147, 290 (2014).
A. Zabiliute, S. Butkute, A. Zukauskas, P. Vitta, and A. Kareiva, 2014. Appl. Optics, 53, 907.
J. Livage, M. Henry, C. Sanchez, 1988. Progr. Solid State Chem. 18, 259.
C. J. Brinker, G. W. Scherrer, 1990. Sol-Gel Science: The Physics and Chemistry of Sol-Gel Processing, Academic Press, San Diego.
B. L. Cushing, V. L. Kolesnichenko, and C. J. O'Connor, 2004. Chem. Rev. 104, 3893.
J. D. Mackenzie, and E. P. Bescher, 2007. Acc. Chem. Res. 40, 810.
N. Dubnikova, E. Garskaite, J. Pinkas, P. Bezdicka, A. Beganskiene, A. Kareiva, 2010. J. Sol-Gel Sci. Techn. 55 (2), p.213 – 219.
E. Garskaite, N. Dubnikova, A. Katelnikovas, J. Pinkas, and A. Kareiva, 2010. Collect. Czech. Chem. Commun. 72, 321.
Xia Li, Hong Liu, Jiyang Wang, Hongmei Cui, Shunliang Yang, I.R. Boughton, 2005. J. Phys. Chem. Solids 66 201-205.
Xia Li, Hong Liu, Jiyang Wang, Hongmei Cui, Feng Han, 2004. J. Am. Ceram. Soc., 87 [12] 2288-2290.
Lin Xing, Luming Peng, Min Gu, Guodong Tang, 2004. J. Alloys Comp. 491 599-604.
Nathalie Pralad, Genevieve Chadeyron, Audrey Potdevin, Jerome Deschamps, Rachid Mahiou, 2013. J. Eur. Ceram. Soc. 33 1935-1945.
R. Skaudzius, A. Zalga, and A. Kareiva, 2008. Materials Science - Medziagotyra 14, 193.
G.Seeta Rama Raju, S. Buddhudu, 2008. Mater. Lett. 62 1259.
Jin Young Park, Hong Chae Jung, G. Seeta Rama Raju, Byung Kee Moon, Jung Hyun Jeong, Jung Hwan Kim. 2010. J. Lumin. 130 478 – 482.
R. Srinivasan, R. Yogamalar, A. Chandra Bose, 2010. Meter. Res Bull. 45.
J. Dhanaraj, R. Jagannathan, T.R.N. Kutty, C.-Hsin Lu, 2001. J. Phys. Chem. B 105 11098.
P.Packiyaraj, P. Thangadurai, 2014. J. Lumin 145 997-1003.
S. K. Singh, Dong Gi Lee, Soung Soo Yi, Kiwan Jang, Dong-Soo Shi, Jung Hyun Jeong, 2013. J. Appl. Phys. 113, 173504.
Redenka M., Krsmanovič Whiffen, Željka Antic, Adolfo Speghini, Mikhail G. Brik, Barbora Bartova, Marco Bettinelli, Miroslav D. Dramicanin, 2014. Opt. Mater. 36 1083-1091.
P.Packiyaraj, P. Thangadurai, 2014. J. Lumin 145 997-1003.
R. E.Muenchausen, L. G. Jacobsohn, B. L. Bennett, E. A. McKigney, 2007. J. F. Smith, J. A. Valdez, D. W. Cooke, J. Lumin, 126 838.